Inverse problems in random media: a kinetic approach

Guillaume Bal

Department of Applied Physics and Applied Mathematics, Columbia University, New York NY, 10027, U.S.A.

E-mail: gb2030@columbia.edu

Abstract. We consider the validity and accuracy of kinetic equations to model the propagation of high frequency waves in highly heterogeneous media. The kinetic models are used to infer the macroscopic properties of the heterogeneous media from wave energy measurements or field-field correlation measurements. We illustrate the theory by considering the imaging of buried inclusions and present reconstructions based on numerical simulations and experimental data.

1. Introduction

This paper summarizes recent work by the author on the propagation of high frequency waves in highly heterogeneous media and related inverse problems. Although the theories presented here apply to other types of equations such as the Maxwell equations of electromagnetism, the equations of elasticity, the Schrödinger and Dirac equations of quantum mechanics, we concentrate on the simpler equations of acoustics. In its simplest form, the propagation of acoustic waves in a heterogeneous medium may be modeled by the following wave equation:

$$\begin{aligned} &\frac{\partial^2 p_\varepsilon}{\partial t^2} - c_\varepsilon^2(\mathbf{x})\Delta p_\varepsilon = 0, && t>0,\ \mathbf{x}\in\mathbb{R}^d,\\ &p_\varepsilon(0,\mathbf{x}) = p_{\varepsilon 0}(\mathbf{x}), \quad \varepsilon\frac{\partial p_\varepsilon}{\partial t}(0,\mathbf{x}) = j_{\varepsilon 0}(\mathbf{x}), && \mathbf{x}\in\mathbb{R}^d, \end{aligned} \tag{1}$$

where $p_\varepsilon(t,\mathbf{x})$ is the pressure potential and $c_\varepsilon(\mathbf{x})$ is the sound speed.

The parameter ε is defined as the ratio of the typical wavelength λ in the system with the overall distance L of the system over which propagation is observed. This is modeled by assuming that e.g. $p_{\varepsilon 0}(\mathbf{x}) = \phi_p(\mathbf{x})\psi_p(\frac{\mathbf{x}}{\varepsilon})$ and $j_{\varepsilon 0}(\mathbf{x}) = \phi_j(\mathbf{x})\psi_j(\frac{\mathbf{x}}{\varepsilon})$ for some smooth functions $\phi_{p,j}(\mathbf{x})$ and $\psi_{p,j}(\mathbf{x})$. We are interested in the regime where $\varepsilon \ll 1$.

In the so-called weak coupling regime, one of the main regimes of wave propagation we consider in this paper, we assume that the sound speed $c_\varepsilon(\mathbf{x})$ takes the form

$$c_\varepsilon^2(\mathbf{x}) = c_0^2(\mathbf{x}) - \sqrt{\varepsilon}V\big(\mathbf{x},\frac{\mathbf{x}}{\varepsilon}\big), \tag{2}$$

where $c_0^2(\mathbf{x})$ is the deterministic background speed and $V(\mathbf{x},\frac{\mathbf{x}}{\varepsilon})$ denotes the rapid oscillations. This shows that the typical wavelength of the propagating waves is comparable to the correlation length l_c of the random medium (the scale at which the heterogeneous medium

fluctuates) so that $\varepsilon = \frac{\lambda}{L} \sim \frac{l_c}{L}$. The low density regime, where the correlation length is much larger than the wavelength will be considered in section 2.

To account for the possible presence of a buried inclusion, we may assume that the wave equation in (1) holds on $\mathbb{R}^d \backslash \overline{D}$, where D is an open, bounded, subset in $\mathbb{R}^d$, and that boundary conditions are prescribed for p_ε on ∂D, for instance $p_\varepsilon = 0$ for sound-soft inclusions and $\frac{\partial p_\varepsilon}{\partial n} = 0$ for unpenetrable inclusions. We may also model the presence of the inclusion as a rapid and local fluctuation in the background sound speed $c_0(\mathbf{x})$.

Several inverse problems may then be considered, where one tries to reconstruct the constitutive parameter of the wave equation $c_\varepsilon(\mathbf{x})$ and the buried inclusions from redundant information such as measurements of the wave fields at the domain's boundary. Many theoretical results exist on the uniqueness of the reconstruction of constitutive parameters in the wave equation from redundant measurements. We refer the reader to the monograph [36] for reconstructions when $\varepsilon = O(1)$. Such results become intractable when $\varepsilon \ll 1$ as it becomes increasingly difficult to reconstruct $V(\mathbf{x}, \frac{\mathbf{x}}{\varepsilon})$ at the fine scale ε. Some approximations are necessary. When the fluctuations are very small, namely $V \ll 1$, then classical reconstructions based on the wave equation in a homogeneous medium may be used with good accuracy. When the initial conditions in (1) are slowly varying, i.e., when $p_{0\varepsilon}$ and $\varepsilon^{-1} j_{0\varepsilon}$ are independent of ε, then homogenization techniques may be used to show that p_ε is well-approximated by the solution to the unperturbed wave equation; see e.g. [7, 38, 40, 47] for the theory of homogenization in random media.

As soon as V becomes large and the initial conditions $p_{0\varepsilon}$ and $j_{0\varepsilon}$ oscillate at the scale ε, then p_ε no longer solves a wave equation in a homogeneous medium, even approximately. The scattering resulting from the high frequency waves interacting with the high frequency random medium becomes dominant. Initial data with high frequencies of order ε^{-1} are the waves we consider in this paper. Lower frequencies provide additional information and should certainly be used in the reconstructions whenever available. We focus here on the information that may be retrieved from measurements of waves with frequencies comparable to ε^{-1}.

Recent theories have been developed in the regime of high frequency initial conditions, which are used to obtain good spatial resolution in the reconstructions when the random fluctuations are sufficiently small so that wave propagation in a homogeneous medium can be used as a forward model but sufficiently large so that classical imaging techniques of wave propagation, such as Kirchhoff migration, fail to provide accurate results. We refer the reader to e.g. [22, 23] for the method of interferometric imaging. The method is based on using functionals of the measured wave fields that are as independent of the realization of the random medium as possible while preserving good resolution capabilities.

When the transport mean free path, the mean distance between successive interactions of the waves with the underlying structure, becomes sufficiently small, then the model of wave propagation in a homogeneous medium breaks down and the accuracy of reconstructions based on such forward models degrades. In such environments, another model of wave propagation becomes necessary, and we claim that the simplest and most natural such model is that of the kinetic equations, which we considered in the following sections.

In this setting, the fine scale oscillations of the speed fluctuations $V(\mathbf{x}, \frac{\mathbf{x}}{\varepsilon})$ are no longer accessible. We are able to observe only the macroscopic features of such fluctuations. It is often reasonable to assume that $V(\mathbf{x}, \mathbf{y})$ is a random field $V(\mathbf{x}, \mathbf{y}; \boldsymbol{\omega})$, where $\boldsymbol{\omega} \in \Omega$, the state space of possible realizations of the heterogeneous medium constructed so that $(\Omega, \mathcal{F}, \mathbb{P})$ is a probability space. We assume here that for each fixed $\mathbf{x}$, $V(\mathbf{x}, \mathbf{y}; \boldsymbol{\omega})$ is a stationary, mean-zero, random field, with a correlation function defined by

$$R(\mathbf{x}, \mathbf{y}) = \mathbb{E}\{V(\mathbf{x}, \mathbf{z}) V(\mathbf{x}, \mathbf{z} + \mathbf{y})\}, \tag{3}$$

where $\mathbb{E}$ is mathematical expectation with respect to $\mathbb{P}$ and where R is independent of $\mathbf{z}$

by stationarity of V. The correlation function $R(\mathbf{x}, \mathbf{y})$ is the only macroscopic, fluctuation-dependent parameter that will appear in the macroscopic models we consider below.

When the fine scale structure cannot be retrieved, the most general inverse problem we can consider thus corresponds to the reconstruction of the macroscopic parameters $c_0(\mathbf{x})$, $R(\mathbf{x}, \mathbf{y})$, and the parameters modeling possible buried inclusions, from knowledge of various measurement operators. Before performing any inversion, we need to find *measurable quantities* and a *macroscopic model* that relates the above constitutive parameters to the measurable quantities. In this paper, we consider two types of measurable quantities: wave energy densities and field-field correlation functions. Section 2 recalls the macroscopic kinetic models that these quantities satisfy in the limit of vanishing wavelength $\varepsilon \to 0$. We describe the kinetic equations in time-dependent and steady-state frameworks for the weak-coupling regime of random fluctuations in (2) and the low-density regime of random fluctuations in (21) below.

In order to be observable in practical experiments, these measurable quantities need to be *statistically stable*. Statistical stability quantifies how stable the measurements are with respect to changes in the realization of the random medium $\boldsymbol{\omega}$. We show in section 3 that wave energy densities and field-field correlations are indeed statistically stable in the sense that their standard deviation is small as the small parameter ε tends to 0. Unfortunately, the available mathematical proofs of statistical stability require that we consider simplified models of wave propagation compared to (1). More importantly, the statistical stability increases when the observables are integrated over larger angular and spatial domains. This has important consequences on the resolution one can expect in reconstructions. We present recent results quantifying these instabilities in the Itô-Schrödinger regime of wave propagation.

The macroscopic description of statistically stable observable quantities allows us to use the macroscopic kinetic models to infer the statistical properties of the constitutive parameters in the wave equation (1). Several relevant results in *inverse transport theory* are recalled in section 4. We insist on two features of inverse transport theory: (i) Observables are more stable statistically after angular averaging. Yet the stability of the reconstruction of kinetic parameters from angular measurements is a severely ill-posed problem. There is therefore an important trade-off in the inversion: lowering the noise level in the measurements requires that sufficient spatial and angular averaging take place, while such averaging degrades the theoretical stability estimates available in inverse transport theory; and (ii) Energy density and field-field correlations behave differently in different scattering regimes. In the imaging of buried inclusions in highly scattering environments, we show that field-field correlations provide higher signal to noise ratios than energy measurements.

These theoretical results allow us to propose in section 5 several reconstruction scenarios based on available measurement data. Because statistical stability requires enough averaging and averaging results in severely ill-posed problems, devising strategies that can increase the signal to noise ratio (SNR) becomes primordial. We consider two ways of increasing the SNR compared to plain wave energy measurements: (i) use differential measurements, and (ii) use field-field correlation measurements.

We illustrate the theoretical predictions by performing numerical simulations of waves in random media and presenting reconstructions of inclusions from experimental data obtained in the micro-wave regime. We assume here that the background speed c_0 is constant and known and that the power spectrum $\hat{R}$ (the Fourier transform of R in the second variable) is also constant but unknown. We then assume that a single spherical inclusion with unknown volume and location is buried in the random medium. We present several numerical simulations and reconstructions from experimental data in this simplified setting.

2. Kinetic models

Kinetic models for the wave energy density. Let us consider the solution $p_\varepsilon(t, \mathbf{x})$ to (1) when the initial conditions oscillate at frequencies of order ε^{-1}. The local energy density of the

waves is given by

$$\mathcal{E}_\varepsilon(t,\mathbf{x}) = \frac{1}{2}\Big(\frac{1}{c_\varepsilon^2(\mathbf{x})}\Big(\varepsilon\frac{\partial p_\varepsilon}{\partial t}\Big)^2(t,\mathbf{x}) + |\mathbf{u}_\varepsilon|^2(t,\mathbf{x})\Big), \tag{4}$$

where $\varepsilon\frac{\partial p_\varepsilon}{\partial t}$ is the pressure field and $\mathbf{u}_\varepsilon = -\varepsilon\nabla_{\mathbf{x}} p_\varepsilon$ is the acoustic velocity field. Up to multiplication by a constant density ρ_0, the first term above is the potential energy and the second term the kinetic energy. The total energy is an invariant of the dynamics so that

$$\mathcal{E}(t) = \int_{\mathbb{R}^d} \mathcal{E}_\varepsilon(t,\mathbf{x})d\mathbf{x} = \mathcal{E}(0) = \int_{\mathbb{R}^d} \frac{1}{2}\Big(\frac{1}{c_\varepsilon^2(\mathbf{x})}|j_{0\varepsilon}|^2(\mathbf{x}) + \big|\varepsilon\nabla_{\mathbf{x}} p_{0\varepsilon}\big|^2(\mathbf{x})\Big). \tag{5}$$

All quantities are rescaled so that $\mathcal{E}(t)$ is of order $O(1)$ independent of ε.

As frequency increases and $\varepsilon \to 0$, the local oscillations of $p_\varepsilon(t,\mathbf{x})$ become less relevant. Rather, one would like to obtain a macroscopic description for the observable energy density $\mathcal{E}_\varepsilon(t,\mathbf{x})$. As in the description of localized quantum waves by classical particles, the energy density does not possess any simple characterization in the physical domain. As particles are classically represented by their position and velocity, then so does the energy density admit a representation in the phase space of positions and momenta:

$$\lim_{\varepsilon\to 0} \mathcal{E}_\varepsilon(t,\mathbf{x}) = \int_{\mathbb{R}^d} a(t,\mathbf{x},d\mathbf{k}), \tag{6}$$

where $a(t,d\mathbf{x},d\mathbf{k})$ is a measure on $\mathbb{R}^{2d}$ for each time $t \geq 0$. In the absence of random fluctuations, $V \equiv 0$, the measure a satisfies the following Liouville equation:

$$\frac{\partial a}{\partial t} + \nabla_{\mathbf{k}}\omega\cdot\nabla_{\mathbf{x}} a - \nabla_{\mathbf{x}}\omega\cdot\nabla_{\mathbf{k}} a = 0, \tag{7}$$

where $\omega(\mathbf{x},\mathbf{k}) = c_0(\mathbf{x})|\mathbf{k}|$ is the Hamiltonian of the dynamics. The Liouville equation (7) is augmented with initial conditions at $t = 0$ that follow (6); see e.g. [35] for the derivation of (7). The high frequency wave packets are approximated by particles whose dynamics are now given by the Hamiltonian system of equations:

$$\dot{\mathbf{X}}(t) = \nabla_{\mathbf{k}}\omega(\mathbf{X}(t),\mathbf{K}(t)), \qquad \dot{\mathbf{K}}(t) = -\nabla_{\mathbf{x}}\omega(\mathbf{X}(t),\mathbf{K}(t)). \tag{8}$$

In the presence of random fluctuations, $V \neq 0$, the wave packets interact with the underlying structure so that scattering is generated. The Liouville equation (7) no longer holds and propagation in a homogeneous medium is no longer an accurate model. Note that the dispersion relation $\omega(\mathbf{x},\mathbf{k}) = c_0(\mathbf{x})|\mathbf{k}|$, which is an invariant of the Liouville equation, relates the temporal and spatial properties of the oscillatory wave fields p_ε. More precisely, in the case of a constant background $c_0(\mathbf{x}) = c_0$, a wave field of the form

$$p_\varepsilon(t,\mathbf{x}) = \phi(t,\mathbf{x})e^{-i\frac{1}{\varepsilon}(\omega t - \mathbf{k}\cdot\mathbf{x})},$$

will satisfy that $\omega = \omega(\mathbf{x},\mathbf{k}) = c_0|\mathbf{k}|$, whereas the amplitude $\phi(t,\mathbf{x})$ will be transported according to the Liouville equation [50]. The dispersion relation is the most basic property of wave packets and modifying it requires very strong fluctuations in the random medium. Modifying the transport properties of the wave packets, however, requires a lesser amount of perturbation. Following these remarks, the role of kinetic models is thus precisely to preserve the dispersion relation of the wave fields while accounting for the scattering generated by the random fluctuations by modifying the transport equation (7) and thus how energy transports.

The simplest way of modifying the transport of energy while preserving the dispersion relation yields the following kinetic model:

$$\frac{\partial a}{\partial t} + \nabla_{\mathbf{k}}\omega\cdot\nabla_{\mathbf{x}} a - \nabla_{\mathbf{x}}\omega\cdot\nabla_{\mathbf{k}} a = \int_{\mathbb{R}^d} \sigma(\mathbf{x},\mathbf{k},\mathbf{q})\big(a(t,\mathbf{x},\mathbf{q}) - a(t,\mathbf{x},\mathbf{k})\big)\delta\big(\omega(\mathbf{x},\mathbf{q}) - \omega(\mathbf{x},\mathbf{k})\big)d\mathbf{k}, \tag{9}$$

where the scattering coefficient is given by:

$$\sigma(\mathbf{x},\mathbf{k},\mathbf{q}) = \frac{\pi\omega^2(\mathbf{x},\mathbf{k})}{2(2\pi)^d}\hat{R}(\mathbf{x},\mathbf{k}-\mathbf{q}). \tag{10}$$

Here, $\hat{R}(\mathbf{x},\mathbf{k})$ is the Fourier transform of the correlation $R(\mathbf{x},\mathbf{z})$ with respect to the second variable only, where the Fourier transform is defined with the convention $\hat{f}(\mathbf{k}) = \int_{\mathbb{R}^d} e^{-i\mathbf{k}\cdot\mathbf{x}} f(\mathbf{x})d\mathbf{x}$. The scattering kernel on the right-hand side of (9) provides the amount of energy that scatters from one direction $\mathbf{q}$ to another direction $\mathbf{k}$ while the dispersion relation $\omega(\mathbf{x},\mathbf{k}) = \omega(\mathbf{x},\mathbf{q})$ is preserved (elastic scattering).

The mathematically rigorous derivation of radiative transfer equations of the form in (9) from first principles is known only in a few settings; see [30, 44]. The derivation of kinetic models from wave equations in similar settings may be found e.g. in [9, 12, 31]. Formal derivations for fairly general hyperbolic (systems of) equations may be found in e.g. [6, 48, 50]. For other regimes of propagation of waves in random media, see e.g. [33, 34, 37, 39, 51].

Note that the above transport equation does not involve any randomness. Its solution is purely deterministic. Since $\mathcal{E}_\varepsilon(t,\mathbf{x})$ in (4) is random, it remains to characterize the sense in which the limit in (6) is considered. We delay these considerations to the next section where issues of statistical stability are considered.

Kinetic models for field-field correlations. Kinetic models are traditionally used to describe the propagation of particles in scattering media. In some sense, the limit (6) describes how the energy density of high frequency wave packets is approximated by a particle evolving in a scattering medium, so that the density of particles (in the phase space) is a solution to (9). We would like to stress that similar kinetic models may be used for more general field-field correlations. Let us consider two heterogeneous media modeled by two sound speeds $c_{\varepsilon,k}(\mathbf{x})$ for $k = 1, 2$ and let $p_{\varepsilon,k}(t,\mathbf{x})$ be the corresponding solutions to the wave equation (1), possibly with different initial conditions. We can then define the following field-field correlation function:

$$\mathcal{C}_\varepsilon(t,\mathbf{x}) = \frac{1}{2}\Big(\frac{1}{c_{\varepsilon,1}(\mathbf{x})c_{\varepsilon,2}(\mathbf{x})}\varepsilon\frac{\partial p_{\varepsilon,1}}{\partial t}\varepsilon\frac{\partial p_{\varepsilon,2}}{\partial t}(t,\mathbf{x}) + \varepsilon\nabla_{\mathbf{x}}p_{\varepsilon,1}\cdot\varepsilon\nabla_{\mathbf{x}}p_{\varepsilon,2}(t,\mathbf{x})\Big). \tag{11}$$

When the two wave fields are identical, the correlation $\mathcal{C}_\varepsilon = \mathcal{E}_\varepsilon$ satisfies the decomposition (6), where a solves (9). There are several possible applications where the two fields $p_{\varepsilon,k}$ may be different and may propagate in different media. For instance, in the monitoring of a turbulent atmosphere, one may have access to measurements at different times. Cross-correlating such measurements provides information about the temporal dynamics of the turbulent atmosphere. We shall see in section 4 that correlations may also provide larger signal to noise ratios than measurements based on energy densities. For an application of such correlations to the analysis of time reversed waves in changing heterogeneous media, see e.g. [20, 43].

Let us assume that the sound speeds are given by

$$c^2_{\varepsilon,k}(\mathbf{x}) = c_0^2(\mathbf{x}) - \sqrt{\varepsilon}V_k\big(\mathbf{x},\frac{\mathbf{x}}{\varepsilon}\big), \tag{12}$$

so that the background sound speeds are the same in the two media. The fluctuations in the sound speed may differ. We expect the two fields $p_{\varepsilon,k}$ to be well-correlated when the two random media are themselves well-correlated. We show below that this is indeed the case.

Let us define the following cross-correlation functions

$$R_{jk}(\mathbf{x},\mathbf{y}) = \mathbb{E}\{V_j(\mathbf{x},\mathbf{z})V_k(\mathbf{x},\mathbf{z}+\mathbf{y})\}, \tag{13}$$

and let $\hat{R}_{jk}(\mathbf{x},\mathbf{k})$ be the Fourier transform of $R_{jk}(\mathbf{x},\mathbf{y})$ with respect to the second variable only. Following [6], we obtain that

$$\lim_{\varepsilon\to 0}\mathcal{C}_\varepsilon(t,\mathbf{x}) = \int_{\mathbb{R}^d} a_{12}(t,\mathbf{x},d\mathbf{k}), \tag{14}$$

where $a_{12}(t,\mathbf{x},\mathbf{k})$ solves the following radiative transfer equation

$$\begin{aligned} &\frac{\partial a_{12}}{\partial t} + \nabla_{\mathbf{k}}\omega\cdot\nabla_{\mathbf{x}}a_{12} - \nabla_{\mathbf{x}}\omega\cdot\nabla_{\mathbf{k}}a_{12} + (\Sigma(\mathbf{x},\mathbf{k}) + i\Pi(\mathbf{x},\mathbf{k}))a_{12} \\ = &\int_{\mathbb{R}^d}\sigma(\mathbf{x},\mathbf{k},\mathbf{q})a_{12}(t,\mathbf{x},\mathbf{q})\delta\big(\omega(\mathbf{x},\mathbf{q})-\omega(\mathbf{x},\mathbf{k})\big)d\mathbf{k}, \end{aligned} \tag{15}$$

where we have defined the following kinetic parameters:

$$\begin{aligned} \Sigma(\mathbf{x},\mathbf{k}) &= \frac{\pi\omega^2(\mathbf{x},\mathbf{k})}{2(2\pi)^d}\int_{\mathbb{R}^d}\frac{\hat{R}_{11}+\hat{R}_{22}}{2}(\mathbf{x},\mathbf{k}-\mathbf{q})\delta\big(\omega(\mathbf{x},\mathbf{k})-\omega(\mathbf{x},\mathbf{q})\big)d\mathbf{q} \\ i\Pi(\mathbf{x},\mathbf{k}) &= \frac{i}{4(2\pi)^d}\text{p.v.}\int_{\mathbb{R}^d}\big(\hat{R}_{11}-\hat{R}_{22}\big)(\mathbf{x},\mathbf{k}-\mathbf{q})\sum_{\pm}\frac{\pm\omega(\mathbf{x},\mathbf{k})\omega(\mathbf{x},\mathbf{q})}{\omega(\mathbf{x},\mathbf{k})-\pm\omega(\mathbf{x},\mathbf{q})}d\mathbf{q} \\ \sigma(\mathbf{x},\mathbf{k},\mathbf{q}) &= \frac{\pi\omega^2(\mathbf{x},\mathbf{k})}{2(2\pi)^d}\hat{R}_{12}(\mathbf{x},\mathbf{k}-\mathbf{q}). \end{aligned} \tag{16}$$

The so-called total absorption parameter $\Sigma(\mathbf{x},\mathbf{k})$ is thus the average of the total absorptions of the random media $k=1$ and $k=2$. The scattering coefficient σ is now proportional to the correlation function of the two random media $\hat{R}_{12}$. When the two random media are perfectly correlated, then the scattering operator becomes that in (9), which is a conservative operator (energy may change from direction $\mathbf{k}$ to direction $\mathbf{q}$ but is conserved overall as $\int_{\mathbb{R}^{2d}} a(t,\mathbf{x},\mathbf{k})d\mathbf{x}d\mathbf{k}$ is an invariant of (9)). When the two random media are no longer perfectly correlated, the absorption term $\Sigma(\mathbf{x},\mathbf{k})$ remains high independent of that correlation. The amount of scattering into other directions, however, decreases with the cross-correlation parameter $\hat{R}_{12}$. High values of $\hat{R}_{12}$ generate a large amount of scattering, which in turns increases the smoothness of the solution $a_{12}(t,\mathbf{x},\mathbf{k})$, in the sense that the smooth high-order scattering component dominates the less smooth low-order scattering component. It is shown in [17] that this smoothness is the very factor that explains why time reversed signals focus tightly in regimes of wave propagation where the kinetic models are valid. Such a result explains for instance why time reversed waves no longer refocus tightly when the random medium changes before waves are back-propagated [20, 43], and thus why imaging in heterogeneous media based on back-propagation of measured signals degrades when the random medium is not known exactly or worse replaced by a homogeneous medium (in which case $\hat{R}_{12}=0$).

Kinetic models for stationary equations. Thus far, we have considered evolution equations to model the propagation of acoustic waves. In many experimental settings, including those described lated in the paper, it is more convenient to model the waves as time harmonic waves. We model the propagation of time harmonic acoustic waves with frequency $\frac{\omega}{\varepsilon}$ by the following Helmholtz equation:

$$\varepsilon^2\Delta u_\varepsilon(\mathbf{x}) + \frac{\omega^2}{c_\varepsilon^2(\mathbf{x})}u_\varepsilon(\mathbf{x}) = \frac{1}{\varepsilon^{\frac{d-1}{2}}}\varphi\Big(\frac{\mathbf{x}-\mathbf{x}_0}{\varepsilon}\Big), \tag{17}$$

where $\varphi(\mathbf{x})$ is a smooth source term localized in the vicinity of a point $\mathbf{x}_0$. We assume that $c_0(\mathbf{x})=c_0$ is constant to simplify so that $\nabla_{\mathbf{k}}\omega(\mathbf{x},\mathbf{k}) = c_0\hat{\mathbf{k}}$ with $\hat{\mathbf{k}}=\frac{\mathbf{k}}{|\mathbf{k}|}$. Following [16], we show that

$$\lim_{\varepsilon\to 0}|u_\varepsilon(\mathbf{x})|^2 = \int_{\mathbb{R}^d} a(\mathbf{x},\mathbf{k})d\mathbf{k}, \tag{18}$$

where the phase space density $a(\mathbf{x}, \mathbf{k})$ solves the following radiative transfer equation

$$c_0 \hat{\mathbf{k}} \cdot \nabla a + \Sigma(\mathbf{x}, \mathbf{k}) a = \int_{\mathbb{R}^d} \sigma(\mathbf{x}, \mathbf{k}, \mathbf{q}) a(\mathbf{x}, \mathbf{q}) \delta(c_0|\mathbf{k}| - c_0|\mathbf{q}|) d\mathbf{q} + Q(\mathbf{x}, \mathbf{k}). \tag{19}$$

The source term is given by

$$Q(\mathbf{x}, \mathbf{k}) = \frac{c_0^3}{4\omega^2 (2\pi)^{d-1}} \delta(\mathbf{x} - \mathbf{x}_0) \delta\Big(\frac{\omega}{c_0} - |\mathbf{k}|\Big) |\hat{\varphi}(\mathbf{k})|^2, \tag{20}$$

while the kinetic parameters σ and Σ are as before.

Weak coupling regime and low density regime. So far we have assumed that the sound speed fluctuations were of the form given in (2). Such fluctuations have small amplitude of order $O(\sqrt{\varepsilon})$ and very small correlation length, $l_c = \varepsilon L$. They are referred to as the weak coupling regime. Although the amplitude of these fluctuations is small, they appear sufficiently often so as to have an effect of order $O(1)$ on the propagating waves. This effect is measured by the mean free path $l = c_0 \Sigma^{-1}$, which is of order $O(1)$ and which measures the mean distance between successive interactions of the energy density with the underlying structure.

Another practically relevant type of random fluctuations that combine to provide order $O(1)$ mean free paths is that of lower-density larger-amplitude scatterers. Such random media were analyzed in [16]. Let us consider a collection of point scatterers $\mathbf{x}_j^\varepsilon(\boldsymbol{\omega})$ given by a Poisson point process of density $\nu_\varepsilon = \varepsilon^{\gamma d} n_0$ for some $0 < \gamma < 1$ and rescaled density $n_0 > 0$. The points $\mathbf{x}_j^\varepsilon(\boldsymbol{\omega})$ should be seen as the centers of the scatterers. Let us assume to simplify that all scatterers have the same velocity profile up to a random multiplicative factor τ_j and define $\mathcal{V}(\mathbf{x})$ a compactly supported, non-negative, uniformly bounded, function. We replace the fluctuations in (2) by

$$\sqrt{\varepsilon} V_\varepsilon(\mathbf{x}, \frac{\mathbf{x}}{\varepsilon}) = \chi(\mathbf{x}) \varepsilon^{\frac{1-(\gamma+\beta)d}{2}} \sum_j \tau_j \mathcal{V}\Big(\frac{\mathbf{y} - \mathbf{x}_j^\varepsilon}{\varepsilon^\beta}\Big)\Big|_{\mathbf{y}=\frac{\mathbf{x}}{\varepsilon}}. \tag{21}$$

The process τ_j is a mean-zero, square integrable, process chosen independent of the Poisson point process. The function $\chi(\mathbf{x})$ indicates the intensity of the fluctuations at the macroscopic scale $\mathbf{x}$. The above expression means that we consider scatterers with a density $n_\varepsilon = \varepsilon^{-d} \nu_\varepsilon = \varepsilon^{(\gamma-1)D} \gg 1$, with a correlation length $l_c = \varepsilon^{1-\gamma} L$, and whose thickness is given by $\varepsilon^{1+\beta} \ll \varepsilon$. The scatterers may thus be modeled by point scatterers since their width is much smaller than the wavelength.

The amplitude of the scatterers may now be of order $O(1)$ provided that e.g. $\beta = \gamma = \frac{1}{2d}$. Their thickness and density has to be chosen to make sure that the resulting mean free path is of order $O(1)$. Following [16], we find that the optical parameters are given by

$$\begin{aligned} \sigma(\mathbf{x}, \mathbf{k}, \mathbf{q}) &= \frac{\pi}{2(2\pi)^d c_0^2} |\mathbf{k}|^2 |\hat{\mathcal{V}}(\mathbf{0})|^2 \mathbb{E}\{\tau^2\} n_0 \chi^2(\mathbf{x}), \\ \Sigma(\mathbf{x}, |\mathbf{k}|) &= \frac{|S^{d-1}| \pi}{2(2\pi)^d c_0^3} |\mathbf{k}|^{d+1} |\hat{\mathcal{V}}(\mathbf{0})|^2 \mathbb{E}\{\tau^2\} n_0 \chi^2(\mathbf{x}), \end{aligned} \tag{22}$$

where $|S^{d-1}|$ is the measure of the unit sphere in $\mathbb{R}^d$.

We observe that scattering is now isotropic, as it no longer depends on the angle between $\mathbf{k}$ and $\mathbf{q}$. The mean free path, given by $l = c_0 \Sigma^{-1}$ is seen to be inversely proportional to the rescaled density of scatterers n_0 and to the $(d+1)$th power of the wavenumber. Scattering thus increases very rapidly with frequency, as the fourth power of frequency in three dimensions of space. This is referred to as Rayleigh scattering.

The above calculations show that radiative transfer equations arise as a natural perturbation of the Liouville equations, which are valid in the absence of rapid fluctuations. The radiative transfer equations arise for a large variety of heterogeneities, provided that the resulting mean free path is neither too large, in which case the Liouville equations are valid, nor too small, for then other phenomena of wave propagation, such as wave localization [51], may arise.

3. Statistical instabilities

The radiative transfer equations (9), (15), and (19), do not involve the realization of the random medium and their solutions are thus deterministic. It remains to specify how the limits in (6) and (14) are considered. The rigorous results obtained in [30, 44] show the convergence of the ensemble average $\mathbb{E}\{\mathcal{E}_\varepsilon(t,\mathbf{x})\}$ to its limit weakly in space (i.e., after integration in space against a sufficiently smooth test function). Although important physically, such a result would not be sufficient for the purpose of inverse problems. Since only one realization of the random medium is accessible in practice, the measured data could possibly be very far from their ensemble average and the macroscopic model (9) would not provide the right mapping between the constitutive parameters of the transport equation and the available measurements.

It turns out that the asymptotic statistical stability of $\mathcal{E}_\varepsilon(t,\mathbf{x})$ may be established for slightly modified wave equations. We first introduce the Wigner transform of two complex-valued functions f and g at the scale ε:

$$W[f,g](\mathbf{x},\mathbf{k}) = \frac{1}{(2\pi)^d}\int_{\mathbb{R}^d} e^{i\mathbf{k}\cdot\mathbf{y}} f\big(\mathbf{x}-\frac{\varepsilon\mathbf{y}}{2}\big) g^*\big(\mathbf{x}+\frac{\varepsilon\mathbf{y}}{2}\big) d\mathbf{y}. \tag{23}$$

The Wigner transform may be seen as a decomposition over wave numbers of the correlation $f(\mathbf{x})g^*(\mathbf{x})$, since by integrating both sides, we obtain that

$$\int_{\mathbb{R}^d} W[f,g](\mathbf{x},\mathbf{k})d\mathbf{k} = f(\mathbf{x})g^*(\mathbf{x}). \tag{24}$$

Let us define

$$W_\varepsilon(t,\mathbf{x},\mathbf{k}) = \frac{1}{2}\Big(\frac{1}{c_{\varepsilon,1}(\mathbf{x})c_{\varepsilon,2}(\mathbf{x})} W[\varepsilon\frac{\partial p_{\varepsilon,1}}{\partial t}, \varepsilon\frac{\partial p_{\varepsilon,2}}{\partial t}](\mathbf{x},\mathbf{k}) + W[\varepsilon\nabla_{\mathbf{x}} p_{\varepsilon,1}, \varepsilon\nabla_{\mathbf{x}} p_{\varepsilon,2}](\mathbf{x},\mathbf{k})\Big). \tag{25}$$

We verify that the above quantity, which we also call a Wigner transform, is a decomposition over wave numbers of the field-field correlation (11):

$$\mathcal{C}_\varepsilon(t,\mathbf{x}) = \int_{\mathbb{R}^d} W_\varepsilon(t,\mathbf{x},\mathbf{k})d\mathbf{k}.$$

In other words, we are interested in which sense the limit of $W_\varepsilon(t,\mathbf{x},\mathbf{k})$ is equal to $a_{12}(t,\mathbf{x},\mathbf{k})$, the solution of (15).

The results of convergence are essentially the same for energy densities and field-field correlations, even though the analysis of the latter is slightly more involved; compare e.g. [5, 12] and [18] in the paraxial and Itô-Schrödinger regimes of wave propagation and [9] and [19] for the regime of wave propagation where the correlation length of the medium l_c is such that $\varepsilon \ll l_c \ll L$. We thus assume for the rest of the section that $p_{\varepsilon,1} = p_{\varepsilon,2}$ so that

$$\mathcal{E}_\varepsilon(t,\mathbf{x}) = \int_{\mathbb{R}^d} W_\varepsilon(t,\mathbf{x},\mathbf{k})d\mathbf{k}.$$

The main theoretical advantage of the Wigner transform $W_\varepsilon(t,\mathbf{x},\mathbf{k})$ is that it satisfies a closed-form equation [6, 50]. Formal asymptotic expansions developed in [50] allow us to pass to the limit in that equation and obtain the transport equation (9).

One way to show that the full random process $W_\varepsilon(t,\mathbf{x},\mathbf{k})$ converges to $a(t,\mathbf{x},\mathbf{k})$ is to look at the following scintillation function (covariance function):

$$J_\varepsilon(t,\mathbf{x},\mathbf{k},\mathbf{y},\mathbf{p}) = \mathbb{E}\{W_\varepsilon(t,\mathbf{x},\mathbf{k})W_\varepsilon(t,\mathbf{y},\mathbf{p})\} - \mathbb{E}\{W_\varepsilon(t,\mathbf{x},\mathbf{k})\}\mathbb{E}\{W_\varepsilon(t,\mathbf{y},\mathbf{p})\}. \tag{26}$$

A non-vanishing limiting scintillation is responsible for the scintillation of stars whose positions seem to depend on time because the realization of the turbulent atmosphere changes with time. That the scintillation converges to 0 in some appropriate sense has been shown rigorously for several regimes of wave propagation. We have already mentioned the regime where $\varepsilon \ll l_c \ll L$ leading to a limiting Fokker-Planck equation rather than a radiative transfer equation [9, 19]. A similar result has been obtained in the paraxial approximation to the wave equation [12]. The paraxial approximation consists of assuming a privileged direction for the waves, say the $z-$direction, and of neglecting back-scattering in that direction. The approximation thus holds for very narrow beams. The reason why the mathematical analysis is much simplified is that the assumption prevents waves from seeing the same position z twice. Classical techniques of mixing of random processes may then be applied and provide a law-of-large-numbers-type self-averaging that allow us to conclude that $W_\varepsilon(t,\mathbf{x},\mathbf{k})$ converges weakly in $(\mathbf{x},\mathbf{k})$ and in probability as a random process, to its deterministic limit $a(t,\mathbf{x},\mathbf{k})$.

In other words, for $\varphi \in L^2(\mathbb{R}^{2d})$,

$$\int_{\mathbb{R}^{2d}} W_\varepsilon(t,\mathbf{x},\mathbf{k})\varphi(\mathbf{x},\mathbf{k})d\mathbf{x}d\mathbf{k} \xrightarrow{\text{prob.}} \int_{\mathbb{R}^{2d}} a(t,\mathbf{x},\mathbf{k})\varphi(\mathbf{x},\mathbf{k})d\mathbf{x}d\mathbf{k}.$$

In both regimes [9, 12], however, the convergence may be proved when $W_\varepsilon(t,\cdot,\cdot) \in L^2(\mathbb{R}^{2d})$ uniformly in time. Moreover, the test function $\varphi(\mathbf{x},\mathbf{k})$ is not allowed to depend on the small parameter ε.

This shows that the transport measurements $W_\varepsilon(t,\mathbf{x},\mathbf{k})$ or $\mathcal{E}_\varepsilon(t,\mathbf{x})$ after averaging over wavenumbers $\mathbf{k}$ such that $\omega(\mathbf{x},\mathbf{k}) = c(\mathbf{x})|\mathbf{k}|$, are asymptotically *statistically stable* provided that: (i) the energy density is sufficiently smooth, and (ii) measurements are averaged over sufficiently large arrays.

More accurate information on the scintillation may be obtained by further simplifying the regime of wave propagation. Still assuming a narrow beam approximation for the propagating waves and neglecting backscattering in the direction $-z$, we further assume that the random fluctuations are very rapid in the z direction. These very rapid fluctuations may then formally be replaced by their limiting process, namely a Wiener measure. We call the limiting model of wave propagation, a (stochastic) partial differential equation, the Itô-Schrödinger equation and refer the reader to [3, 12] for its derivation. The limiting model describes the propagation of a beam in the main direction z and how the beam widens in the transverse directions $\mathbf{x}$. The main advantage of the Itô-Schrödinger model is that the scintillation (26) becomes the solution of an explicit kinetic equation.

The analysis of the scintillation function was considered in [5] and significantly generalized in [15] in the Itô-Schrödinger regime. The salient feature of these analyzes is that the size of the scintillation function crucially depends on two factors: (i) the regularity of the initial condition for the wave equation; and (ii) the size of the array of measurements. Whether the theoretical results obtained in that simplified regime extend to more challenging models of wave propagation remains to be seen. However, we expect the regularity of the initial conditions and the size of the array of measurements to have a qualitatively similar influence on the scintillation function in more general regimes of wave propagation as well.

Let us summarize some of the results obtained in [5, 15]. A first, negative, result is that the scintillation function does not decay to 0 in the limit $\varepsilon \to 0$ when the initial conditions for the transport equation are $a(0,\mathbf{x},\mathbf{x}) = \delta(\mathbf{x}-\mathbf{x}_0)\delta(\mathbf{k}-\mathbf{k}_0)$. Note that initial conditions for the wave equation may be constructed so that the initial condition of the Wigner transform

converges to the singular measure $\delta(\mathbf{x}-\mathbf{x}_0)\delta(\mathbf{k}-\mathbf{k}_0)$. More precisely, it is shown in [5] that for such initial conditions, the scintillation $J_\varepsilon(t,\mathbf{x},\mathbf{k},\mathbf{y},\mathbf{p})$ is equal to a leading term given by $\delta(\mathbf{x}-\mathbf{y})\delta(\mathbf{k}-\mathbf{p})\alpha(t,\mathbf{x},\mathbf{k})$ plus other components that are mutually singular with respect to that leading term, where the density $\alpha(t,\mathbf{x},\mathbf{k})$ admits an explicit characterization obtained by solving a kinetic equation. This implies that the wave energy density is *not* statistically stable in the limit $\varepsilon \to 0$ and this is a very negative result as far as the inverse transport problem is concerned.

For smoother initial conditions for the wave equation, scintillation indeed decreases to 0 as the wavelength $\varepsilon \to 0$. Following [15], we consider initial conditions for the wave equation in the Itö Schrödinger regime given by

$$\psi_\varepsilon(\mathbf{x}) = \frac{1}{\varepsilon^{\frac{d\alpha}{2}}}\chi\Big(\frac{\mathbf{x}}{\varepsilon^\alpha}\Big)e^{i\frac{\mathbf{x}\cdot\mathbf{k}_0}{\varepsilon}}, \tag{27}$$

where $\chi(\mathbf{x})$ is a smooth function modeling the support of the source and $\mathbf{k}_0$ is the direction of propagation of the wave packet. The scaling is such that the initial condition is bounded in $L^2(\mathbb{R}^d)$ independent of ε. Here d is the spatial dimension of the transverse directions $\mathbf{x}$. More general initial conditions are considered in [15]. Let us now model the array of detectors by

$$\varphi_\varepsilon(\mathbf{x},\mathbf{k}) := \varphi_{\varepsilon,s_1,s_2}(\mathbf{x},\mathbf{k}) = \frac{1}{\varepsilon^{d(s_1+s_2)}}\varphi\Big(\frac{\mathbf{x}}{\varepsilon^{s_1}},\frac{\mathbf{k}-\mathbf{k}_1}{\varepsilon^{s_2}}\Big), \tag{28}$$

with an aperture of size ε^{s_2} in wavenumbers in the vicinity of $\mathbf{k}_1$ and size ε^{s_1} in space in the vicinity of $\mathbf{x}_0 = \mathbf{0}$. The function $\varphi(\mathbf{x},\mathbf{k})$ is assumed to be non-negative and such that $\int_{\mathbb{R}^{2d}}\varphi(\mathbf{x},\mathbf{k})d\mathbf{x}d\mathbf{k} = 1$. Normalization is such that the average of φ_ε is independent of ε.

The scintillation function quantifies the probability that the measurements deviate from the kinetic solution. Using the Chebyshev inequality, we obtain that

$$\mathbb{P}\Big(|\langle W_\varepsilon(t,\mathbf{x},\mathbf{k}),\varphi_\varepsilon\rangle - \langle a(t,\mathbf{x},\mathbf{k}),\varphi_\varepsilon\rangle| \geq \delta\Big) \leq \frac{1}{\delta^2}\Big|\langle J_\varepsilon(t),\varphi_\varepsilon\otimes\varphi_\varepsilon\rangle\Big|. \tag{29}$$

For initial conditions of the form given in (27), we obtain in [15] the following bound for the scintillation function:

$$\Big|\langle J_\varepsilon(t),\varphi_\varepsilon\otimes\varphi_\varepsilon\rangle\Big| \leq C\varepsilon^{(2\alpha-1)\vee 0-2ds_2}\Big(\varepsilon^{d(1-\alpha-2s_1)}\wedge\varepsilon^{d(1-2\alpha-s_1)}\Big), \tag{30}$$

where $a\wedge b = \inf(a,b)$ and $a\vee b = \sup(a,b)$. The above formula shows how scintillation decreases as the size of the array of measurements increases (s_1 and s_2 decrease) and the smoothness of the initial condition increases (α decreases).

Let us assume that $s_2 = 0$ so that the energy density is angularly averaged. For a large array of detectors so that $s_1 = 0$, we find that scintillation is proportional to $\varepsilon^{\alpha+d(1-\alpha)}$. For smooth initial conditions with $\alpha = 0$, we thus obtain the smallest possible value of the scintillation, of order $O(\varepsilon^d)$. This means that the measured random variable $\langle W_\varepsilon,\varphi\rangle$ has a standard deviation proportional to $O(\varepsilon^{\frac{d}{2}})$.

For initial conditions with narrow spatial support and $\alpha = 1$, we obtain that the scintillation is proportional to $O(\varepsilon)$. This means that the measured random variable $\langle W_\varepsilon,\varphi\rangle$ has a standard deviation proportional to $O(\sqrt{\varepsilon})$, which is much larger than the optimal $O(\varepsilon^{\frac{d}{2}})$. Such a bound is in fact optimal as we showed in [15] that $\varepsilon^{-1}J_\varepsilon$ converges in the sense of distributions to a limiting scintillation function solution of an explicit kinetic equation.

Another interesting expression we can derive from (30) pertains to the minimal size of the array of measurements. Let us assume that $\alpha = 0$ so that the source has large support. Then we find that scintillation is bounded by $O(\varepsilon^{d(1-s_1)})$. This result shows that the wave energy measurements are asymptotically statistically stable in the limit $\varepsilon \to 0$ as soon as the array of measurements has a spatial aperture ε^{s_1} that is large compared to the wavelength ε. This result is also optimal as we do not expect any statistical stability of the wave energy density at the scale of the random fluctuations ε.

4. Inverse transport theory

Uniqueness results from knowledge of the albedo operator. The transport equations seen in the preceding sections may be recast as

$$\frac{\partial a}{\partial t} + \boldsymbol{\theta} \cdot \nabla a + \Sigma(\mathbf{x}) a = \int_{S^{d-1}} \sigma(\mathbf{x}, \boldsymbol{\theta}, \boldsymbol{\theta}') a(t, \mathbf{x}, \boldsymbol{\theta}') d\mu(\boldsymbol{\theta}'), \tag{31}$$

after proper rescaling of the wave number $\boldsymbol{\theta} = \frac{\mathbf{k}}{|\mathbf{k}|} \in S^{d-1}$ and $d\mu$ is the standard measure on the unit sphere. We have assumed here that $c_0(\mathbf{x}) = c_0 = 1$ and refer the reader to e.g. [46] for generalizations when the sound speed $c_0(\mathbf{x})$ is also unknown.

We may now probe the scattering medium on a bounded, convex, domain $X \subset \mathbb{R}^d$, $d \geq 2$, by sending information from the domain's boundary and taking measurements of outgoing particles at the domain's boundary. Let us define the sets

$$\Gamma_{\pm} = \{(\mathbf{x}, \boldsymbol{\theta}) \in \partial X \times S^{d-1}, \text{ such that } \pm \mathbf{n}(\mathbf{x}) \cdot \boldsymbol{\theta} > 0\}, \tag{32}$$

where $\mathbf{n}(\mathbf{x})$ is the outward unit normal to X at $\mathbf{x} \in \partial X$, and $d\xi = |\mathbf{n}(\mathbf{x}) \cdot \boldsymbol{\theta}| d\mu(\boldsymbol{\theta}) dS(\mathbf{x})$, where dS is the surface measure on ∂X. For $a_- \in L^1_c(\mathbb{R}; L^1(\Gamma_-, d\xi))$, the above transport equation with conditions $a = a_-$ on $\mathbb{R} \times \Gamma_-$ admits a unique solution and a trace $a_+ = a_{|\Gamma_+}$, which is well defined in $L^1_{\text{loc}}(\mathbb{R}; L^1(\Gamma_+, d\xi))$; see [52]. We then define the albedo operator $\mathcal{A}$, which maps a_- to $a_+ = \mathcal{A} a_-$. It is shown in [27] that $\mathcal{A}$ uniquely determines $\Sigma(\mathbf{x})$ and $\sigma(\mathbf{x}, \boldsymbol{\theta}, \boldsymbol{\theta}')$.

A similar theory holds for the steady state problem, where solutions of (31) of the form $a(\mathbf{x}, \mathbf{k})$ independent of time are sought. Under appropriate smallness assumptions on the scattering coefficient $\sigma(\mathbf{x}, \boldsymbol{\theta}, \boldsymbol{\theta}')$ so that the transport equation is well-posed, it is shown in [28] that the albedo operator, which maps $a_- \in L^1(\Gamma_-, d\xi)$ to $a_{|\Gamma_+} = \mathcal{A} a_- \in L^1(\Gamma_+, d\xi)$, uniquely determines $\Sigma(\mathbf{x})$. In dimensions $d \geq 3$, the scattering coefficient $\sigma(\mathbf{x}, \boldsymbol{\theta}, \boldsymbol{\theta}')$ is also uniquely determined. In dimension $d = 2$, $\sigma(\mathbf{x}, \boldsymbol{\theta}, \boldsymbol{\theta}')$ is uniquely determined provided that it is sufficiently small [53]. Several uniqueness results come with stability analyses; we refer the reader to [52] for more details on the inverse transport theory from knowledge of the full albedo operator.

In both the time dependent and the steady state cases, the unique reconstructions of the optical parameters comes from the following decomposition of the albedo operator:

$$\mathcal{A} = \mathcal{A}_0 + \mathcal{A}_1 + \mathcal{A}_2, \tag{33}$$

where $\mathcal{A}_0$ corresponds to the ballistic part, obtained by setting $\sigma \equiv 0$ in (31), and where $\mathcal{A}_1$ is the part of $\mathcal{A}$ that is linear in σ and thus corresponds to the single scattering contribution to the albedo operator. In all cases, it may be shown that $\mathcal{A}_0$ is more singular (in the sense that its Schwartz kernel is more singular) that the other components of $\mathcal{A}$. We then observe that the $X-$ray transform of $\Sigma(\mathbf{x})$ is uniquely determined by $\mathcal{A}_0$, whence the reconstruction of $\Sigma(\mathbf{x})$ by inverse Radon transform. In dimension $d \geq 3$ for the steady-state problem and in dimension $d \geq 2$ for the time-dependent problem, $\mathcal{A}_1$ is also more singular than $\mathcal{A}_2$ and allows one to uniquely determine $\sigma(\mathbf{x}, \boldsymbol{\theta}, \boldsymbol{\theta}')$.

Reconstructions from averaged measurements. Radiative transfer equations of the form (31) may be used in several applications such as radiation through turbulent atmospheres [26] and clouds [45] and near-infra-red photon propagation in tissues and its applications in optical tomography [2]. In most applications, the full albedo operator is rarely available. Moreover, angularly resolved measurements are rarely feasible, either because they would be too long to acquire or because the amount of energy (or photon count) is too low.

In the propagation of waves in random media, we have seen that there is another important limitation: the statistical instability of the measurements. Localized sources of radiations or

localized measurements in the phase space both result in statistically unstable quantities. It may therefore be more suitable to model available measurements as averaged measurements.

The main theoretical difficulty with averaged measurements is that the singularities of the albedo operator $\mathcal{A}$ are often lost by integration, so that the theories recalled in the preceding paragraph no longer apply. The theory of uniqueness of optical parameters from averaged measurements is less well understood. Consider the following angularly averaged measurements at the domain's boundary:

$$J(\mathbf{x}) = \int_{S^{d-1}} \boldsymbol{\theta} \cdot \mathbf{n}(\mathbf{x}) a(\mathbf{x}, \boldsymbol{\theta}) d\mu(\boldsymbol{\theta}), \tag{34}$$

where $J(\mathbf{x})$ is the current of particles at $\mathbf{x} \in \partial X$. Reconstructions of optical parameters from knowledge of $J(\mathbf{x})$ (rather than $a(\mathbf{x}, \theta)_{|\Gamma_+}$) have recently been addressed in [10, 41]. In [41], it is shown that knowledge of $J(\mathbf{x})$ for all possible $a_{|\Gamma_-}$ (so that the sources are still angularly resolved) allows us to uniquely reconstruct $\Sigma(\mathbf{x})$ and to reconstruct $\sigma(\mathbf{x}, \boldsymbol{\theta}, \boldsymbol{\theta}') = \sigma(\mathbf{x})\phi(\boldsymbol{\theta}, \boldsymbol{\theta}')$ provided that $\sigma(\mathbf{x})$ is sufficiently small and ϕ is known and real analytic. In [10], it is shown that knowledge of $J(\mathbf{x})$ for all possible $a_{|\Gamma_-}(\mathbf{x}, \boldsymbol{\theta}) = f(\mathbf{x})$ (so that sources are no longer angularly resolved) uniquely determines the low-frequency part of $\sigma(\mathbf{x}, \boldsymbol{\theta}, \boldsymbol{\theta}') = \sigma(\mathbf{x})$ provided that $\Sigma(\mathbf{x})$ and $\sigma(\mathbf{x})$ are sufficiently small. Surprisingly, the latter result, which is based on a linearization with respect to σ of the measurement operator, uses the same complex geometrical optics solutions as in the Calderón problem, where the reconstruction of parameters in an elliptic equation is sought [24]. As a consequence, the reconstruction of $\sigma(\mathbf{x})$ from available measurements is shown to be a severely ill-posed problem.

Reconstruction of small-volume inclusions. In the case of averaged measurements, which are necessary in waves in random media if one is to expect to obtain statistically stable data, it is often necessary to have a low-dimensional parameterization of the quantities one aims to reconstruct. One useful, and now well-studied, such parameterization consists of assuming the presence of well-localized small inclusions buried in an underlying medium with smooth coefficients. This parameterization provides a good tool to quantify what type of perturbations can (or cannot) be reconstructed at a given noise level; see [1, 4, 25].

In the context of the imaging of buried inclusions in random media, the reconstruction of small-volume inclusions from energy density and from field-field correlation measurements was recently considered in [13].

We denote by $p_{\varepsilon,1}$ the wave solution in the absence of the inclusion and by $p_{\varepsilon,2}$ the wave solution in the presence of the inclusion. Let us consider inclusions that are either sound-soft or unpenetrable. This translates at the kinetic level as specular boundary conditions for the wave energy density. We thus obtain that the phase-space energy density $a_2(t, \mathbf{x}, \mathbf{k})$ in the presence of the inclusion solves (9) on $\mathbb{R}^d \backslash \overline{D}$, where D is the support of the inclusion, and satisfies the following boundary conditions

$$a_2(t, \mathbf{x}, \mathbf{k}) = a_2(t, \mathbf{x}, \mathbf{k} - 2\mathbf{k} \cdot \mathbf{n}(\mathbf{x})\mathbf{n}(\mathbf{x})), \quad \mathbf{x} \in \partial D, \tag{35}$$

where $\mathbf{n}(\mathbf{x})$ is the outward unit normal to D at $\mathbf{x} \in \partial D$.

Let us now consider the correlation $\mathcal{C}_\varepsilon$ in (11) based on correlating the wave solution $p_{\varepsilon,1}$ in the absence of the inclusion with the wave solution $p_{2,\varepsilon}$ in the presence of the inclusion. At the kinetic level, the limit a_{12} solves the equation (9) on $\mathbb{R}^d \backslash \overline{D}$, since on $\mathbb{R}^d \backslash \overline{D}$, the two random media for $p_{\varepsilon,1}$ and $p_{\varepsilon,2}$ agree. The boundary conditions, however, are now given by

$$a_{12}(t, \mathbf{x}, \mathbf{k}) = 0 \quad \text{in} \quad \mathbf{x} \in D \qquad (\text{and on } \mathbf{x} \in \partial D). \tag{36}$$

The reason why a_{12} vanishes at the inclusion's location may be understood as follows. Let us think of a localized wave packet impinging on the object. In the absence of the inclusion, that

wave packet propagates though D. In the presence of the inclusion, it is specularly reflected. These two wave packets then propagate in different directions and interfere destructively. As a result, their Wigner transform converges (weakly) to 0 with ε and we obtain in the (weak) limit that a_{12} vanishes inside D; see [13] for more details.

Let $a_1(t, \mathbf{x}, \mathbf{k})$ be the solution of the kinetic equation (9) in the absence of the inclusion. Then we can measure the influence of the inclusion on the energy data by looking at $(a_1 - a_2)(t, \mathbf{x}, \mathbf{k})$ for $\mathbf{x} \in \partial X$ where measurements are taken. The influence on the field-field correlation data may be defined as $(a_1 - a_{12})(t, \mathbf{x}, \mathbf{k})$. The main result of the analysis in [13], which borrows from similar analyses in [1, 25], shows that

$$\|a_1 - a_2\|_{L^1} \approx \mathsf{R}^{d-1}, \qquad \|a_1 - a_{12}\|_{L^1} \approx \mathsf{R}^{d-1}, \tag{37}$$

when the mean free path $c_0\Sigma^{-1}$ is of order $O(1)$. Here, R is the radius of the inclusion and the L^1 norm is defined in the space $(\mathbf{x}, \mathbf{k}) \in \mathbb{R}^d \times S^{d-1}$. In such a regime, it may therefore not be worth while measuring field-field correlations.

In the regime of very small mean free paths compared to L (but very large compared to the wavelength so that the kinetic models are still valid with the same stability estimates as those shown before), which corresponds to the high scattering regime, the solution to the transport equation may be well-approximated by the solution to a diffusion equation [29]. In such a regime, it is shown that

$$\|a_1 - a_2\|_{L^1} \approx \mathsf{R}^{d}, \qquad \|a_1 - a_{12}\|_{L^1} \approx \mathsf{R}^{d-2}, \tag{38}$$

for $d \geq 3$, where R^{d-2} above should be replaced by $|\ln \mathsf{R}|^{-1}$ in dimension $d = 2$. Instead of being proportional to its volume, the influence of the inclusion on the correlation data is proportional to its radius in dimension $d = 3$. In scattering media, the measurement of field-field correlations may thus provide significantly higher signal-to-noise ratios than would the measurement of energy densities.

5. Imaging scenarios

In the appropriate regimes of wave propagation, we have obtained macroscopic kinetic models for energy densities and field-field correlations. The constitutive parameters in these kinetic equations are the statistical properties of the heterogeneous media and the properties of the buried inclusions. For the rest of this paper, we consider the following simplified problem, where the random medium is assumed to be statistically invariant by translation, so that the mean free path is independent of position, and where we assume that we have one buried inclusion with a very simple geometry (we shall assume that it is spherically symmetric for concreteness; see [16] for extensions).

We assume that the probing waves are high frequency waves with wavenumbers of order $(L\varepsilon)^{-1}$. We are interested in reconstructing the optical parameters of the medium and the properties of the inclusion from such frequencies.

High frequencies are typically being used because of their resolution capabilities, proportional to the wavelength ε. In the absence of any high frequency fluctuations of the underlying medium, such a resolution may be obtained by back-propagating available data into the homogeneous medium. The back-propagated (time-reversed) waves tightly focus at the inclusion's location with an accuracy of half of a wavelength when a sufficiently large aperture is available. In the presence of *known* high frequency fluctuations in the random medium, the back-propagation of measured waves still provides a very useful imaging tool [21, 32, 34] as it allows for an accuracy of up to half of a wavelength even in the presence of small aperture measurements. The analysis in [20, 43] shows, however, that the random medium need be known extremely accurately for the time reversed waves to refocus at the location of the inclusion.

When the random medium oscillates rapidly and is not known explicitly, which is the case in most applications, the back-propagation of the measured waves will not provide any meaningful reconstruction. Moreover, the reconstructed image will be extremely unstable statistically. In the presence of a limited amount of randomness, this statistical instability may be mitigated in an optimal way by averaging the unknown random fluctuations at a scale that renders the data statistically stable while preserving the highest degree of resolution. This is the method of coherent interferometric imaging [22, 23]. As randomness increases, the spatial resolution at the scale ε degrades. However, so long as the mean free path is sufficiently large, the method provides an optimal degree of resolution.

When the amount of randomness increases to a larger level and the mean free path becomes sufficiently small, the model of propagation in a homogeneous medium may no longer be used. As we have claimed earlier in this paper, the simplest modification for wave propagation in a homogeneous medium is to model the energy density or the field-field correlation of those waves with a kinetic description. Although measurements may be statistically stable in such configurations, they require that the source terms and the arrays of detectors be sufficiently delocalized spatially, and certainly at scales significantly larger than the wavelength. Wavelength resolution is therefore irretrievably lost in such regimes unless additional information is inserted. These facts bring us to the introduction of several possible imaging scenarios.

(i) The first scenario is based on measurements of the energy density $\mathcal{E}_\varepsilon(t, \mathbf{x})$ for an interval of times and on an array of detectors. We do not have access to measurements in the absence of an inclusion. We call these measurements direct measurements.

(ii) The second scenario is based on measurements of the energy density $\mathcal{E}_{\varepsilon,1}(t, \mathbf{x})$ in the absence and $\mathcal{E}_{\varepsilon,2}(t, \mathbf{x})$ in the presence of the inclusion. We call such measurements differential measurements.

(iii) The third scenario is based on measurements of the field-field correlation $\mathcal{C}_\varepsilon$ and of the energy density $\mathcal{E}_{\varepsilon,1}$. This requires us to measure the fields $p_{k,\varepsilon}$ for $k = 1, 2$ accurately to form the correlation $\mathcal{C}_\varepsilon$.

The first scenario is the least demanding technologically. It requires that we measure the energy density, which does not necessitate a measurement accuracy at the level of the wavelength. Also, it does not require that we probe the medium in the absence of the inclusion, which may not be feasible in many applications. This scenario, however, provides measurements of limited quality. Because of the statistical instability presented in section 3, the influence of the inclusion need be significantly larger than the error caused by the uncontrolled instabilities. For not-too-small mean free paths and small inclusions, this means that R^{d-1} need be significantly larger than the instability, which ranges from $\varepsilon^{\frac{d}{2}}$ to almost $O(1)$ depending on the smoothness of the initial conditions and of the array of detectors.

The second and third scenarios are defined to mitigate the influence of the statistical instability on the measurements. In the absence of an inclusion, the difference of energies and the difference of correlations vanish. The resulting statistical instability for these scenarios is therefore proportional to the influence of the object itself. This is a much lower statistical instability than that of scenario (i). The advantage of scenario (iii) over scenario (ii) is that the influence of the object is significantly larger in the former than in the latter when the mean free path is relatively small; see (38).

6. Inversions from numerical and experimental data

Accuracy of time domain kinetic models. The accuracy of the kinetic models in the time domain and the frequency domain has been tested numerically in a series of recent papers [13, 14, 16, 49]. These calculations are computationally fairly intensive as they require that waves propagate through large domains (compared to the wavelength) so that the mixing predicted by theory may occur.

The comparison of simulations of the time dependent wave equation with simulations of the kinetic models were considered in [13, 14]. The wave equation is solved by a finite difference model and the kinetic equation is solved by a Monte Carlo method. The agreement between the exact wave equation and the kinetic prediction is very good. We present a few numerical comparisons in Fig.1, where we consider the influence of inclusions of radius R between 30 and 50 wavelengths on energy density measurements 300 wavelengths away. The mean free paths range between 36 and 88 wavelengths approximately; see [13] for more details.

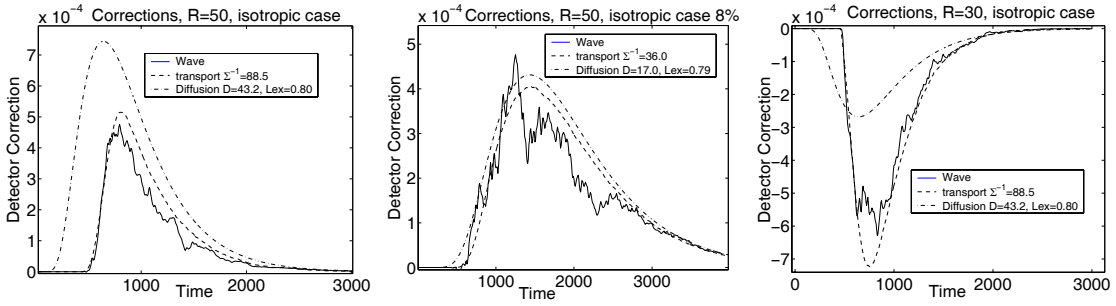

Figure 1. Comparison of wave energy densities obtained by solving the wave equation and the kinetic model. In each case, the energy density is calculated in the presence and in the absence of an inclusion. The resulting difference of energies at the detector's location is plotted as a function of time. From left to right: Void inclusion of radius $\mathsf{R} = 50$ and mean free path of 88 wavelengths; Void inclusion of radius $\mathsf{R} = 50$ and mean free path of 36 wavelengths; Reflecting inclusion of radius $\mathsf{R} = 30$ and mean free path of 71 wavelengths.

In [14], we considered the influence of inclusions of size $\mathsf{R} = 8$ and $\mathsf{R} = 15$ wavelengths on an array of detectors located 150 wavelength away from the inclusion. The source and the detectors are located at the same place. The size of the detector is 40×60 wavelengths, and the random medium has fluctuations of standard deviation 8% of the average sound speed, which result in a mean free path (the sole meaningful quantity to measure the amount of disorder in the random medium) equal to 37 wavelengths. The waves have to travel for 8 mean free paths to probe the inclusion. The kinetic model for the correlation function $\mathcal{C}_\varepsilon$ is as accurate as for the energy densities plotted in Fig.1; see [14]. We want to insist here on the results plotted in Fig.2. The dotted (green) curve represents the relative statistical instability (standard deviation) of the energy measurements as a function of time. It is based on calculations over 20 realizations of the random medium. The relative influence of the inclusion on the energy density is the solid (red) line while the influence of the inclusion on the field-field correlation is the dashed (blue) line.

In both cases, imaging based on scenario (i) would fail because the statistical instability of the measurements is significantly larger than the influence of the object. In scenarios (ii) and (iii), the dotted (green) curve no longer represents the measurement noise. The latter noise may come from taking the difference of large numbers or from external noise. In any case, we observe that the signal to noise ratio is significantly larger for correlation measurements than for energy measurements. Moreover, the presence of an inclusion can only degrade the quality of field-field coherence so that the dashed (blue) curve can only be positive valued, at least on average. In such a regime, we see the clear advantage of reconstructions based on field-field correlations, provided the latter are technologically available.

Reconstructions from time harmonic measurements. The reconstruction of buried inclusions from the time-harmonic kinetic model (19) was studied recently in [16]. We consider a heterogeneous medium composed of tightly localized scatterers modeled as point scatterers.

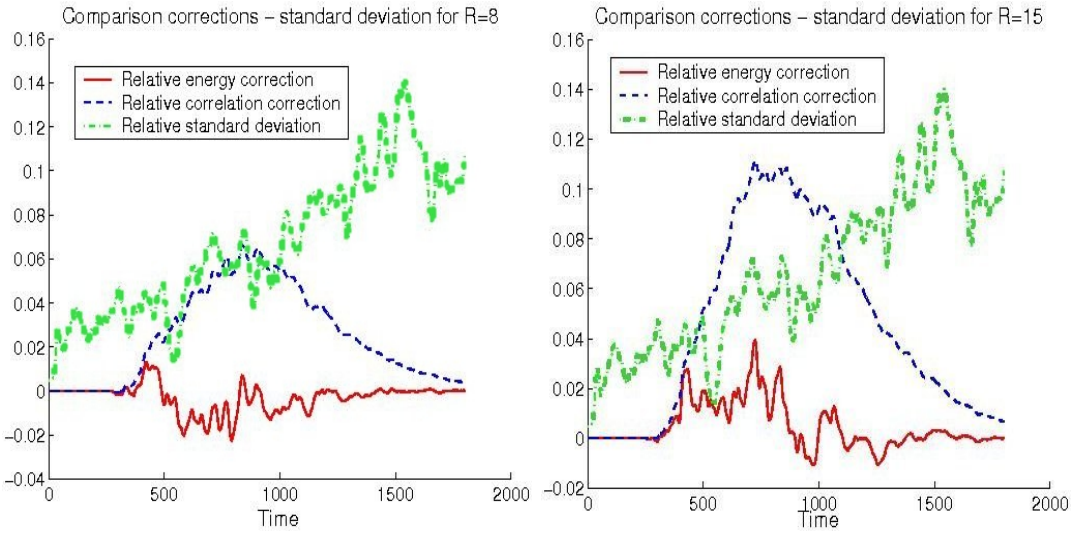

Figure 2. Comparison relative standard deviation - relative correlation correction - relative energy correction, for a mean free path of 37 wavelengths and $\mathsf{R} = 8$ (left) and $\mathsf{R} = 15$ (right).

The Helmholtz equation (17) is thus solved by using a Foldy-Lax model. The kinetic model with parameters given in (22) is solved by a Monte Carlo method. In both the wave and kinetic models, the source term is a delta function in space located outside of the random medium (see below for a pictorial description of the numerical setting).

The statistical instability of the measurements depends on the the size of the array of detectors, as expected, but also on the density of scatterers (at a fixed mean free path). Although theoretical calculations are still under way, we expect fewer and stronger scatterers to generate more unstable measurements than higher densities of weaker scatterers. Such instabilities are confirmed by looking at the comparisons between wave and transport simulations presented in Fig.3.

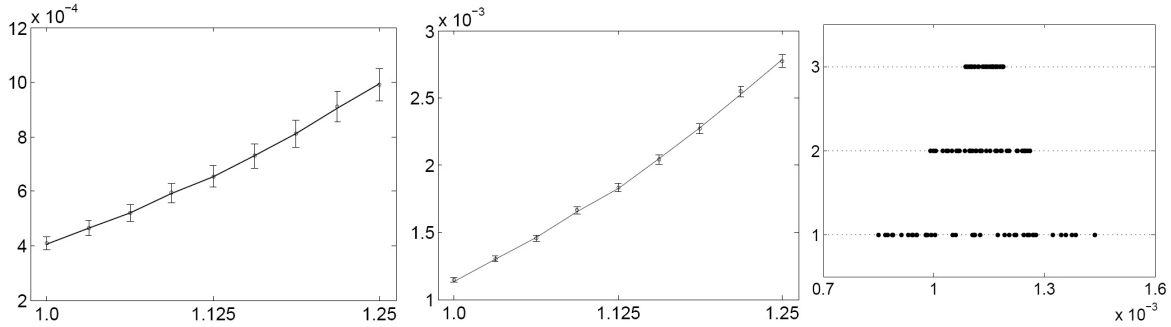

Figure 3. Comparison between measured transport and wave data at frequencies between $\omega = \frac{2\pi}{\lambda}$ and 1.25ω with detectors of size $40\lambda \times 40\lambda$ (left) and $80\lambda \times 80\lambda$ (center), respectively for a mean free path $c_0\Sigma^{-1} = 40\lambda$, where $\lambda(= 1)$ is wavelength. Solid line: transport energy density; Circles with error bar: wave energy density $\mathbb{E}\{\mathcal{E}_\varepsilon\}$ and its standard deviation $\sigma(\mathcal{E}_\varepsilon)$. Right: Statistical stability of wave data with respect to media properties for a mean free path $c_0\Sigma^{-1} = 30\lambda$. Each dot corresponds to the wave energy measured on the array of detectors for one realization with an average of 6000 scatterers (top lines labeled 3; $l_c \approx 3.65\lambda$), 3000 scatterers (middle lines labeled 2; $l_c \approx 5.16\lambda$), and 1500 scatterers (bottom lines labeled 1; $l_c \approx 7.30\lambda$), respectively.

Reconstructions of inclusions inside the random medium, outside the random medium, and hidden behind a blocker were considered in [16]. We focus on the latter configuration presented in Fig.4. The reconstructions are based on differential measurements as described in scenario (ii). In the configuration of a statistically homogeneous background with buried inclusions, the

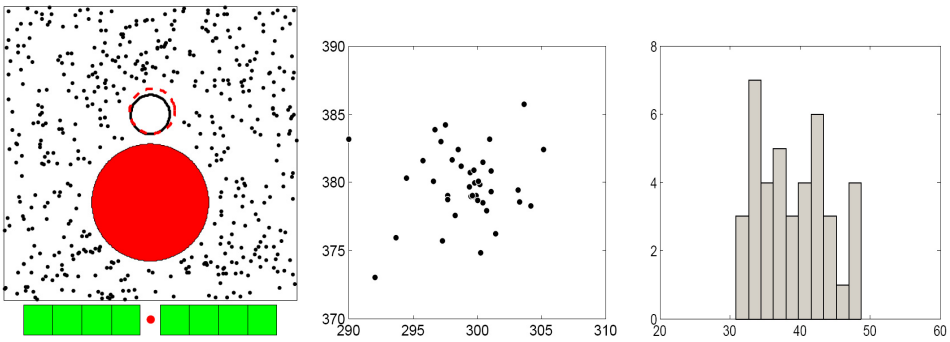

Figure 4. Reconstruction of an inclusion hidden behind a large blocker with $c_0\Sigma^{-1} = 75\lambda$. From left to right: a typical reconstruction (the dashed circle is the reconstructed inclusion), distribution of the reconstructed locations and histogram of the reconstructed radius.

use of high frequency waves may not be optimal to probe the medium. Lower-frequency wave fields would scatter less and consequently provide better imaging capabilities in spite of their lower resolution in homogeneous media. There is a configuration in which high scattering may become necessary: When the line of sight between the source term and the object one wishes to reconstruct is blocked, the reconstruction in weakly-scattering environments relies on the diffraction of waves, which may be extremely faint when the blocker is a smooth object as in Fig.4. The presence of scatterers thus helps to focus energy on the unknown inclusion. All that the radiative transfer model requires is that the number of scatterers be sufficiently large and the resulting mean free path be not too small so that the measurements are relatively stable statistically. We observe that the reconstructed size of the inclusion range from 30 to 50 for a real radius of the inclusion $\mathsf{R} = 40$ wavelengths. Even when differential measurements are available, the statistical instabilities of the energy measurements prevents one from obtaining wavelength-scale resolution.

Reconstruction from experimental data. Let us conclude this section with the reconstruction of inclusions buried in a heterogeneous environment from experimental data in the microwave regime. The results are reported in greater details in [8].

The experiments performed in L.Carin's group at Duke University [8, 43] consist of a forest of 600 dielectric rods with dielectric constant $\epsilon_r = 2.5$. A target was placed beyond the random medium or behind a blocker. In an other experiment, three nearby rods were removed from the random medium. In all cases, the inclusion or void is parameterized by its position and its radius, assuming a cylindrical symmetry. All the reconstructions presented here are based on differential measurements (scenario (ii)) of mono-frequency waves of frequency 10GHz, which corresponds to a wavelength of roughly 3cm. The mean free path is estimated from the energy measurements in the absence of any inclusion. The parameters of the inclusion are then estimated by using the energy differences.

The mean free path in the medium was estimated to be 40cm. The random medium is therefore 2.5 mean free paths thick, which corresponds to significant disorder. The experimental and numerical settings are presented in Fig.5. Energy measurements are performed at 18 equi-distant antennas on the same side of the random medium as the source term. A comparison of the exact inclusions and their reconstructions from the kinetic model are given in Fig.6. Because of the invariance of the geometry in the vertical direction,

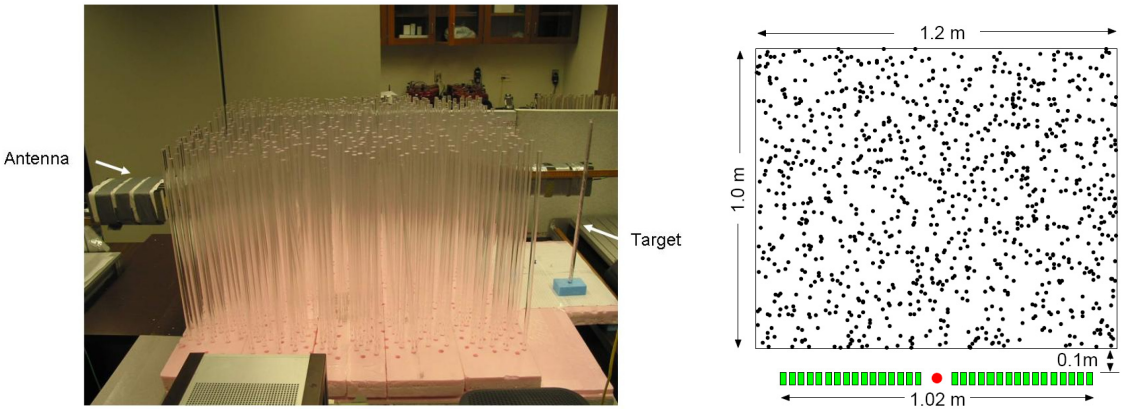

Figure 5. Experimental setting (left) and corresponding Numerical Setting (right)

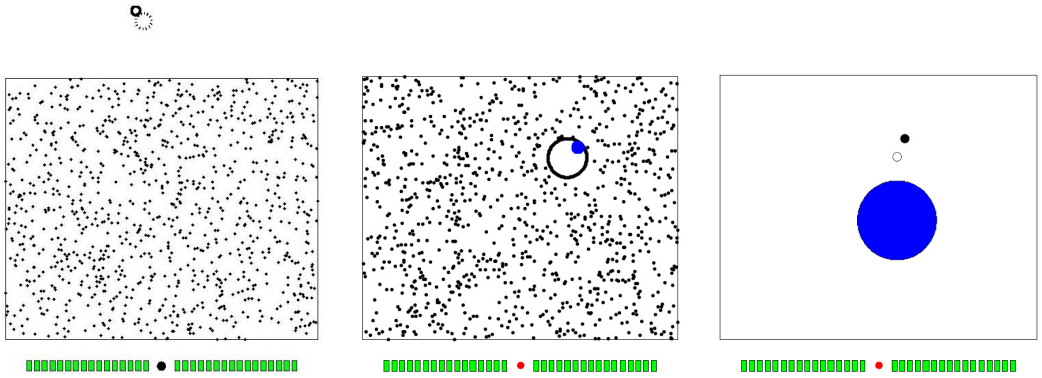

Figure 6. Reconstructions of inclusions (left), voids (center), and inclusions behind a blocker (right). The scatterers have been removed in the latter plot for better readability.

the experimental medium may be modeled as a two-dimensional medium. In the Rayleigh scattering regime, we expect the mean free path to decay as the third power of frequency, a law which was very well reproduced experimentally [8].

The reconstructions of the locations of the inclusions and voids are fairly accurate. The reconstruction of their sizes is less accurate. This is because specular reflections for the energy density were assumed at the boundary of the inclusions. Such assumptions do not hold for small inclusions and should be replaced by a more accurate model for scattering. But overall, the kinetic models perform quite well in a configuration of dielectric scatterers that was not optimized in any way: the scatterers were placed manually to simply *look* random. Note, however, that the reconstructions require that we be given differential data. The size of the inclusions was much too small to allow for any meaningful detection, let alone reconstruction, in the presence of direct data as in scenario (i).

7. Conclusions

Kinetic theories provide an interesting macroscopic model for the propagation of high frequency waves in random media with mean free paths that are neither too large with respect to the overall size of the medium (for then, effective medium theories will work well) nor too small with respect to the wavelength (for then, localization effects or other statistical instabilities dominate the measurements).

These theories have been validated numerically and experimentally in practically relevant situations, where the mean free path is roughly two orders of magnitude larger than the

wavelength and comparable or one order of magnitude smaller than the overall distance of propagation we are interested in, such as e.g. twice the distance between a source term/detector array and a localized inclusion.

The statistical instability as measured for instance by the size of the scintillation function is now well-understood in several regimes of wave propagation. The size of the scintillation function is the main limiting factor in the accuracy of the kinetic models to solve inverse problems. We have a quantitative understanding of the size of scintillation as a function of the regularity of the array of detectors and of the source term. Although the theory is not yet complete, we have a qualitative understanding of the scintillation as a function of the density of scatterers in the heterogeneous medium.

The inverse transport theory that best models these instabilities consists of assuming that only spatially or angularly averaged measurements are available. Although inverse transport theories from full measurements are now well-understood, inverse transport theories based on partial and averaged measurements remain fairly incomplete.

The resolution one can hope for in regimes of validity of kinetic models is much lower than that in the absence of small scale heterogeneities. Wavelength-scale resolution is no longer available and resolution degrades as the frequency increases because scattering increases as well. The detection and reconstruction of small objects thus requires us to obtain differential measurements, i.e., measurements in the presence and in the absence of a perturbation. In the regime of fairly high scattering, field-field correlations provide much higher signal to noise ratios than energy measurements do.

Although we have focused here on the reconstruction of localized inclusions, the same inverse problems allow us to reconstruct spatially varying optical parameters, as is the case in e.g. optical tomography. Applications of such inverse problems include the analysis and monitoring of turbulent atmospheres probed by acoustic or electromagnetic waves, or the analysis of structure in the earth crust probed by seismic waves.

In such applications, it may be useful to consider additional properties of the waves to their intensity. Kinetic equations for electromagnetic waves model the full Stokes vectors, which account for possible polarization of the waves [6, 50]. Polarization measurements of electromagnetic and elastic waves allow for much better practical reconstructions of the underlying medium; see e.g. [11]. To the best of the author's knowledge, the theoretical analysis of vector-valued transport equations has not been done yet.

Acknowledgments

I would like to thank my collaborators over the years for their help in appreciating the difficulties inherent to the modeling of waves in random media and to inverse transport theory: Larry Carin, Tomasz Komorowski, Ian Langmore, George Papanicolaou, François Monard, Miguel Moscoso, Olivier Pinaud, Kui Ren, Lenya Ryzhik, and Ramón Verástegui. My warmest thanks to Gunther Uhlmann for organizing and inviting me to the IAP 2007 conference in Vancouver. The work was funded in part by DARPA-ONR grant N00014-04-1-0224 under the Mathematical Time Reversal program directed by Carey Schwartz and in part by the National Science Foundation under Grants DMS-0239097 and DMS-0554097.

References

[1] H. Ammari and H. Kang, *Reconstruction of Small Inhomogeneities from Boundary Measurements*, Lecture Notes in Mathematics, Springer, Berlin, 2004.

[2] S. R. Arridge, *Optical tomography in medical imaging*, Inverse Problems, 15 (1999), pp. R41–R93.

[3] F. Bailly, J. F. Clouet, and J.-P. Fouque, *Parabolic and gaussian white noise approximation for wave propagation in random media*, SIAM J. Appl. Math, 56(5) (1996), pp. 1445–1470.

[4] G. Bal, *Optical tomography for small volume absorbing inclusions*, Inverse Problems, 19 (2003), pp. 371–386.

[5] ———, *On the self-averaging of wave energy in random media*, Multiscale Model. Simul., 2(3) (2004), pp. 398–420.
[6] ———, *Kinetics of scalar wave fields in random media*, Wave Motion, 43 (2005), pp. 132–157.
[7] ———, *Homogenization in random media and effective medium theory for high frequency waves*, Disc. Cont. Dyn. Syst. B, 8 (2007), pp. 473–492.
[8] G. Bal, L. Carin, D. Liu, and K. Ren, *Experimental validation of a transport-based imaging method in highly scattering environments*, Inverse Problems, 23(6) (2007), pp. 2527–2539.
[9] G. Bal, T. Komorowski, and L. Ryzhik, *Self-averaging of Wigner transforms in random media*, Comm. Math. Phys., 242(1-2) (2003), pp. 81–135.
[10] G. Bal, I. Langmore, and F. Monard, *Inverse transport with isotropic sources and angularly averaged measurements*, Inverse Probl. Imaging, 2(1) (2008), pp. 23–42.
[11] G. Bal and M. Moscoso, *Polarization Effects of Seismic Waves on the Basis of Radiative Transport Theory*, Geophys. J. Int., 142(2) (2000), pp. 571–585.
[12] G. Bal, G. C. Papanicolaou, and L. Ryzhik, *Self-averaging in time reversal for the parabolic wave equation*, Stochastics and Dynamics, 4 (2002), pp. 507–531.
[13] G. Bal and O. Pinaud, *Accuracy of transport models for waves in random media*, Wave Motion, 43(7) (2006), pp. 561–578.
[14] ———, *Kinetic models for imaging in random media*, Multiscale Model. Simul., 6(3) (2007), pp. 792–819.
[15] ———, *Self-averaging of kinetic models for waves in random media*, Kinetic Related Models, 1 (2008), pp. 85–100.
[16] G. Bal and K. Ren, *Transport-based imaging in random media*, submitted, (2008).
[17] G. Bal and L. Ryzhik, *Time Reversal and Refocusing in Random Media*, SIAM J. Appl. Math., 63(5) (2003), pp. 1475–1498.
[18] ———, *Stability of time reversed waves in changing media*, Disc. Cont. Dyn. Syst. A, 12(5) (2005), pp. 793–815.
[19] ———, *Wave field correlations in weakly mismatched random media*, Stochastics & Dynamics, 6(3) (2006), pp. 301–328.
[20] G. Bal and R. Verástegui, *Time Reversal in Changing Environment*, Multiscale Model. Simul., 2(4) (2004), pp. 639–661.
[21] P. Blomgren, G. C. Papanicolaou, and H. Zhao, *Super-Resolution in Time-Reversal Acoustics*, J. Acoust. Soc. Am., 111(1) (2002), pp. 230–248.
[22] B. Borcea, G. C. Papanicolaou, and C. Tsogka, *Theory and applications of time reversal and interferometric imaging*, Inverse Problems, 19 (2003), pp. S139–S164.
[23] ———, *Adaptive interferometric imaging in clutter and optimal illumination*, Inverse Problems, 22 (2006), pp. 1405–1436.
[24] A. Calderón, *On an inverse boundary value problem*, Seminar on Numerical Analysis and its Applications to Continuum Physics, Soc. Brasileira de Matematica, Rio de Janeiro, (1980), pp. 65–73.
[25] D. J. Cedio-Fengya, S. Moskow, and M. S. Vogelius, *Identification of conductivity imperfections of small diameter by boundary measurements. Continuous dependence and computational reconstruction*, Inverse Problems, 14 (1998), pp. 553–594.
[26] S. Chandrasekhar, *Radiative Transfer*, Dover Publications, New York, 1960.
[27] M. Choulli and P. Stefanov, *Inverse scattering and inverse boundary value problems for the linear Boltzmann equation*, Comm. Partial Diff. Equ., 21 (1996), pp. 763–785.
[28] ———, *Reconstruction of the coefficients of the stationary transport equation from boundary measurements*, Inverse Problems, 12 (1996), pp. L19–L23.
[29] R. Dautray and J.-L. Lions, *Mathematical Analysis and Numerical Methods for Science and Technology. Vol.6*, Springer Verlag, Berlin, 1993.
[30] L. Erdös and H. T. Yau, *Linear Boltzmann equation as the weak coupling limit of a random Schrödinger Equation*, Comm. Pure Appl. Math., 53(6) (2000), pp. 667–735.
[31] A. Fannjiang, *Self-averaged scaling limits for random parabolic waves*, Archives of Rational Mechanics and Analysis, 175(3) (2005), pp. 343–387.
[32] M. Fink, *Time reversed acoustics*, Physics Today, 50(3) (1997), pp. 34–40.
[33] J.-P. Fouque, (ed.) *Diffuse Waves in Complex Media*, Kluwer, Dordrecht, The Netherlands, 1999.
[34] J.-P. Fouque, J. Garnier, G. Papanicolaou, and K. Sølna, *Wave Propagation and Time Reversal in Randomly Layered Media*, Springer, New York, 2007.
[35] P. Gérard, P. A. Markowich, N. J. Mauser, and F. Poupaud, *Homogenization limits and Wigner transforms*, Comm. Pure Appl. Math., 50 (1997), pp. 323–380.
[36] V. Isakov, *Inverse Problems for Partial Differential Equations*, Springer Verlag, New York, 1998.
[37] A. Ishimaru, *Wave Propagation and Scattering in Random Media*, New York: Academics, 1978.
[38] V. V. Jikov, S. M. Kozlov, and O. A. Oleinik, *Homogenization of differential operators and integral functionals*, Springer-Verlag, New York, 1994.

[39] J. B. Keller, *Stochastic equations and wave propagation in random media*, in Proc. Sympos. Appl. Math., Vol. XVI, Amer. Math. Soc., Providence, R.I, 1964, pp. 145–170.
[40] S. M. Kozlov, *The averaging of random operators*, Math. USSR Sb., 109 (1979), pp. 188–202.
[41] I. Langmore, *The stationary transport equation with angularly averaged measurements*, submitted, (2007).
[42] P.-L. Lions and T. Paul, *Sur les mesures de Wigner*, Rev. Mat. Iberoamericana, 9 (1993), pp. 553–618.
[43] D. Liu, S. Vasudevan, J. Krolik, G. Bal, and L. Carin, *Electromagnetic time-reversal imaging in changing media: Experiment and analysis*, IEEE Trans. Antennas and Prop., 55 (2007), pp. 344–354.
[44] J. Lukkarinen and H. Spohn, *Kinetic limit for wave propagation in a random medium*, Arch. Ration. Mech. Anal., 183 (2007), pp. 93–162.
[45] A. Marshak and A. B. Davis, *3D Radiative Transfer in Cloudy Atmospheres*, Springer, New-York, 2005.
[46] S. McDowall, *Optical Tomography on simple Riemannian surfaces*, Comm. Partial Diff. Eqs., (2005), pp. 1379–1400.
[47] G. C. Papanicolaou and S. R. S. Varadhan, *Boundary value problems with rapidly oscillating random coefficients*, in Random fields, Vol. I, II (Esztergom, 1979), Colloq. Math. Soc. János Bolyai, 27, North Holland, New York, 1981, pp. 835–873.
[48] J. M. Powell and J. Vanneste, *Transport equations for waves in randomly perturbed Hamiltonian systems, with application to Rossby waves*, Wave Motion, 42 (2005), pp. 289–308.
[49] J. Przybilla, M. Korn, and U. Wegler, *Radiative transfer of elastic waves versus finite difference simulations in two-dimensional random media*, J. Geoph. Res. Solid Earth, 111 (2006), p. B04305.
[50] L. Ryzhik, G. C. Papanicolaou, and J. B. Keller, *Transport equations for elastic and other waves in random media*, Wave Motion, 24 (1996), pp. 327–370.
[51] P. Sheng, *Introduction to Wave Scattering, Localization and Mesoscopic Phenomena*, Academic Press, New York, 1995.
[52] P. Stefanov, *Inside Out: Inverse problems and applications*, vol. 47 of MSRI publications, Ed. G. Uhlmann, Cambridge University Press, Cambridge, UK, 2003, ch. Inverse Problems in Transport Theory.
[53] P. Stefanov and G. Uhlmann, *Optical tomography in two dimensions*, Methods Appl. Anal., 10 (2003), pp. 1–9.